AGE RELATIONSHIPS OF LARGE-SCALE TROUGHS AND IMPACT BASINS ON VESTA. Hiu Ching Jupiter Cheng[1], Christian Klimczak[1] and Caleb I. Fassett[2], [1]Structural Geology and Geomechanics Group, Department of Geology, University of Georgia, Athens, GA 30602, USA (jupiterchc@uga.edu). [2]NASA Marshall Space Flight Center, 320 Sparkman Drive, Huntsville, AL, 35805, USA

Introduction: The Dawn mission [1] at asteroid 4 Vesta revealed two sets of enormous troughs with one set spanning around two-thirds of the equator and the other set located in the northern hemisphere. It has been shown that the equatorial and northern troughs are concentric around the Rheasilvia and Veneneia impact basins, respectively [2]. This spatial relationship is the main argument for the two sets of troughs to be formed directly by, and simultaneously with the basin-forming impacts. However, the temporal relationships of the troughs and how they compare to the impact basins have never been documented.

Methodology: We counted crater populations superposed on the equatorial and northern troughs using the buffered crater counting technique and compared those to crater counts derived for the Rheasilvia and Veneneia basins, respectively. We conducted mapping used ESRI ArcGIS software with the CraterTools [3], which has a built-in buffered crater-counting function [4]. The definition of count areas and mapping of superposed craters was performed on the Dawn FC images with a resolution of ~60 m/pixel [5], and assisted by the use of ~93 m/pixel digital terrain model [6].

The count area of equatorial and northern troughs are defined by a linear depression bounded by two scarps where sharp surface breaks are observed on the topographic profiles facing each other. Only craters that directly superpose troughs within the count areas were counted. Crater statistics of the troughs were computed using the buffered crater-counting technique [e.g., 4, 7]. Given the thin and indistinct ejecta for craters on Vesta, we used a buffer equal to the crater radius (or 0.5*D*; where *D* denotes crater diameter). The effective count areas were computed for each crater depending on their size, allowing the creating of a size-frequency determination at all measured crater sizes.

We also conducted crater counting in selected count areas within the Veneneia and Rheasilvia basins. In particular, we duplicated the count area defined by [8], including the top of the central peak of the Rheasilvia basin and the eastern part of the Veneneia basin to avoid underestimating their formation timing due to potential resurfacing on the basin floor. Superposing craters were mapped for these count areas, and crater frequencies were then computed with the conventional technique.

We generated data as *cumulative frequencies* in a standard root-2 crater diameter binning. The plots display the integral of $N(D)$, in which $N(D)$ is the cumulative number of the craters equal to or larger than a given diameter, *D*, normalized to a count area. Uncertainties were calculated based on Poisson counting statistics with a 90% confidence level in gamma cumulative distribution. We derived *absolute ages* by applying the lunar-like crater production and chronology functions for Vesta based on the Dawn parameters [8].

Equatorial troughs and Rheasilvia basin: The equatorial troughs mapping yield an unbuffered count area of 18780 km^2, outlining the best-preserved trough portions. Crater counts were completed with 1034 craters in total ranging from 0.6 km up to ~19 km in diameter, which were analyzed with the buffered crater count technique. The duplicated count area from [8] at the top of the Rheasilvia central peak is 458 km^2 with 31 craters between 0.6 and 8 km in diameter.

The crater statistics are presented in Fig 1. The cumulative size-frequency distribution of the equatorial troughs exhibits a relatively constant slope and has robust counting statistics for craters with $D \geq 2$ km. However, the frequencies deficient in smaller craters below D =~2 km. For the top of the Rheasilvia basin peak, the cumulative size-frequency distribution exhibits a reasonably constant slope for craters with $D \geq 2$ km. Again, a kink occurs at $D = 2$ with a sub-production slope for smaller craters. The absence of craters with $D \geq 8$ km superposed on the Rheasilvia central peak is directly attributable to the small count area, which contributes to poor counting statistics at the larger crater diameters.

Comparing the crater statistics of equatorial troughs and the Rheasilvia basin (Fig. 1) enables us to determine their temporal relationships. The equatorial troughs generally have a lower estimated frequency than the Rheasilvia central peak. However, based on the frequency uncertainties in most of the bins, it is not possible to determine if the two landforms differ in age. Given that the cumulative crater size-frequencies of the equatorial troughs mostly overlap with the lower bound of the uncertainties of frequencies of the Rheasilvia central peak, the equatorial troughs could be coeval with or somewhat post-date the surface age of the Rheasilvia central peak.

We determine the absolute age of each of the troughs and basin by fitting the lunar-like production function [8] to the cumulative frequency distribution in the crater size range that exhibits a more or less constant slope. Craters of ≥2 km in diameter give the best fit to the predicted production population and yield an

interpreted model age for the equatorial troughs of ~3.3 Ga with N(2) = 1.14×10^{-2} km^{-2} and Rheasilvia basin to be ~3.5 Ga with N(2) = 1.53×10^{-2} km^{-2}, confirming the model age from [8]. The derived absolute age for the equatorial toughs yields an average ~200 Ma younger age than that of the surface of the central peak of the Rheasilvia basin.

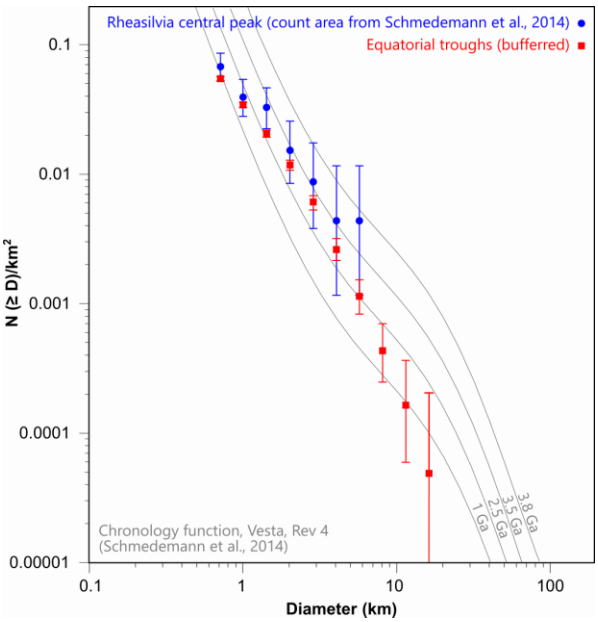

Figure 1. Cumulative size-frequency distributions of equatorial troughs and Rheasilvia basin.

Northern troughs and Veneneia basin: An unbuffered count area of 11689 km^2 was mapped for two northern troughs. A total of 1038 craters ranging from 0.6 km up to ~20 km in diameter were mapped in the area and analyzed with the buffered crater count technique. The count area of the eastern Veneneia basin floor was duplicated from [8], yielding a size of 20058 km^2. Counts were completed with 1035 craters ranging from 0.6 up to ~23 km in diameter.

The crater statistics of the northern troughs and eastern Veneneia basin are presented in Fig. 2. The eastern Veneneia basin exhibits a cumulative size-frequency distribution with a constant slope plotting between the production functions of 2.5 Ga and 3.5 Ga for most of the bins but is deficient in smaller craters of $D \leq 2$km. The best-fit model age for craters $D \geq 2$ km superposed in the count area of the Veneneia basin confirms the absolute age derived from [8] of ~3.1 Ga, with $N(2) = 9.67\times10^{-3}$ km^{-2}. These crater counts are not meaningful for interpretation of the emplacement age of the basin because the Rheasilvia basin superposes the Veneneia basin [2], so the Veneneia basin-forming impact must predate that of Rheasilvia at ~3.5 Ga.

The cumulative size-frequency distribution of the northern troughs exhibits a reasonably constant slope for $D \geq 2$ km, with frequencies of $D \geq 8$ km plotting below and smaller craters plotting above the 3.5 Ga isochron. The best-fit absolute age for the northern troughs with $D \geq 2$ km is ~3. 6 Ga for $N(2)$ 2.80×10^{-2} km^{-2}.This absolute age is older than that of the Rheasilvia basin, which is consistent with the hypothesized origin of the troughs.

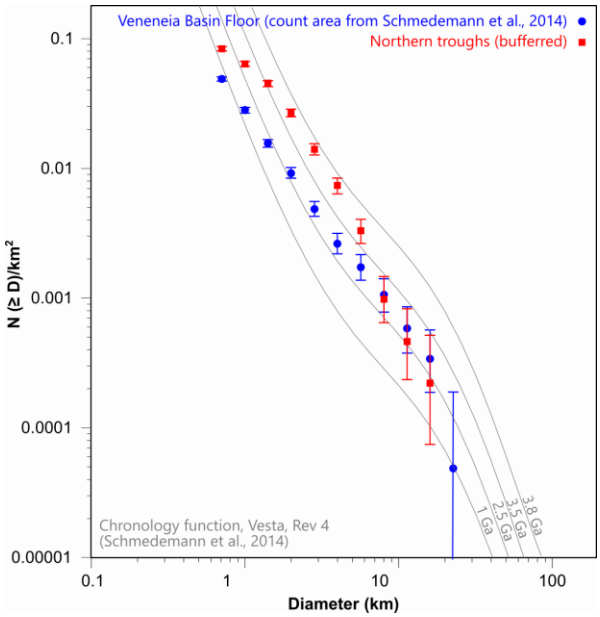

Figure 2. Cumulative size-frequency distributions of northern troughs and Veneneia basin.

Conclusions: We documented age relationships between the large troughs and impact basins on Vesta. Our results do not contradict but also do not yield tight constraints on the hypothesis that the basin-forming impacts directly triggered the formation of troughs on Vesta.

References: [1] Russell, C. T., & Raymond, C. A. (2011). Springer. [2] Jaumann, R. et al. (2012). Science, 336(6082), 687-690. [3] Kneissl, T. et al. (2011). Planetary and Space Science, 59(11-12), 1243-1254. [4] Kneissl, T. et al. (2015). Icarus, 250, 384-394. [5] Sierks, H. et al. (2011). Space Science Reviews, 163(1-4), 263-327. [6] Gaskell, R. W. (2012). DPS Meeting, pp. 209-03. [7] Fassett, C. I., & Head III, J. W. (2008). Icarus, 198(1), 37-56. [8] Schmedemann, N. et al. (2014). Planetary and Space Science, 103, 104-130.